Proceedings RootS25
3rd International Workshop on Soil-Vegetation-Atmosphere Interaction
Boldrin D, Cecconi M, Cotecchia F, Leung A, Pedone G, Perrini P, Romero E, Tagarelli V, Zdravković L (eds)
ISSN: 3107-300X

doi: doi.org/10.53243/RootS2025-3

Coupling hyperelasticity with bounding surface plasticity for constitutive modeling of fiber-reinforced soils

Nazanin Irani[1], Torsten Wichtmann[1]

[1]*Chair of Soil Mechanics, Foundation Engineering, and Environmental Geotechnics, Ruhr-University Bochum, Bochum, Germany*

ABSTRACT: A promising approach to simulating root-reinforced soils involves first developing a constitutive model for fiber-reinforced soils, which can later be extended to account for suction effects. However, most existing models for fiber-reinforced soils are not formulated within a thermodynamically consistent framework. As a result, they may predict non-recoverable energy and stress responses under closed strain cycles and cyclic loading. Root reinforcement is widely employed in slope stability applications, where slopes are frequently subjected to repeated loading/unloading due to seismic activity, intense rainfall, and traffic-induced vibrations. Accurately capturing the cyclic behavior of these soils is essential, as such loading can progressively degrade soil structure, leading to cumulative deformations, reductions in shear strength, and potential triggering of liquefaction. In response to these challenges, this study introduces a novel hyperelastic-plastic constitutive model for fiber-reinforced soils. The elastic frame is formulated using a free energy function, thereby ensuring energy conservation. The resultant hyperelasticity is then coupled with a bounding surface plasticity to predict irreversible response in a hyperelastic-plastic frame. Furthermore, a new state parameter is proposed to account for the influence of fiber inclusion on the stress-dilatancy behavior of soils. The model is validated at the element level through comparisons with experimental data.

Keywords: Fiber-reinforcement; Hyperelastic-plastic model; Thermodynamic laws; Bounding surface plasticity

1 INTRODUCTION

Vegetation plays a vital role in the stability and resilience of geotechnical systems, particularly through the reinforcing effect of plant roots within the soil matrix (Karimzadeg et al., 2021). Root-reinforced soils have been widely recognized as an environmentally sustainable and cost-effective alternative to conventional soil stabilization techniques in applications such as slope stabilization, erosion control, and shallow landslide prevention. The reinforcing action of roots enhances soil shear strength by providing additional tensile resistance, interlocking, and anchorage, while also potentially improving soil permeability and hydrological balance (Gao and Zhao, 2013). These benefits are particularly critical in regions prone to rainfall-induced slope failures and in infrastructures subjected to long-term serviceability demands. Consequently, the ability to realistically simulate the mechanical behavior of root-reinforced soils is of paramount importance for advancing sustainable geotechnical design and risk assessment.

Despite their recognized importance, modeling the mechanical behavior of root-reinforced soils remains challenging due to the inherent complexity of soil–root interactions, including heterogeneity in root distribution, anisotropy, and the coupled effects of suction and hydro-mechanical processes. A promising strategy to address these complexities might be to draw an analogy between root reinforcement and fiber reinforcement in soils (Mair Wood et al., 2016). Fiber reinforcement introduces discrete tensile elements that act within the soil skeleton, improving its ductility and post-peak strength (Ganiev et al., 2022). Similarly, root networks provide comparable reinforcement by bridging soil particles and mobilizing tensile forces under shear deformation. Thus, constitutive models developed for fiber-reinforced soils provide a benchmark framework that can be extended to root-reinforced systems, after which hydrological effects need to be incorporated. Nevertheless, most available constitutive models for fiber-reinforced soils are not formulated within a thermodynamically consistent framework (Irani et al., 2025). This limitation has significant implications for practical simulations: under cyclic or repeated loading conditions—such as those induced by seismic shaking, traffic vibrations, or fluctuating pore pressures during heavy rainfall—such models may predict spurious stress paths, non-recoverable energy dissipation, and unrealistic hysteretic responses. Given that root-reinforced soils are often employed in slopes exposed to such cyclic disturbances, these shortcomings hinder reliable predictions of long-term performance.

In light of these challenges, the present study develops a novel hyperelastic–plastic constitutive model for fiber-reinforced soils as a foundation for simulating root reinforcement.

2 CONSTITUTIVE FRAMEWORK

The proposed constitutive framework integrates a hyperelastic formulation with bounding surface plasticity. In this concept, soil behavior is represented as energy-conservative in the small-strain regime (typically for strains below 10^{-4}), where the response is governed purely by hyperelasticity. Once the stress state reaches the yield surface, plastic mechanisms are activated, and the material response transitions to a coupled hyperelastic–plastic regime. The hyperelastic component is derived from a rigorously defined energy potential, ensuring thermodynamic consistency, while the plastic response is formulated using the bounding surface plasticity theory of Dafalias and Manzari (2004). To capture reinforcement effects, additional terms accounting for fiber–soil interactions are embedded within the plasticity framework. The fundamental constitutive equations of the proposed model are expressed in the following sub-sections.

In terms of basic notation, tensor-valued quantities are denoted in boldface. The double-dot operator ":" between two tensors indicates a contracted product, i.e., summation over adjacent pairs of indices in reverse order. For the case of second-order tensors, this reduces to the standard trace operation. Specifically, for two second-order tensors $\boldsymbol{A}$ and $\boldsymbol{B}$, the operation is defined as $tr(\boldsymbol{AB}) = \boldsymbol{A}:\boldsymbol{B} = A_{ij}B_{ij}$.

2.1 Hyperelasticity

To characterize the elastic response, the energy potential Ψ is formulated in terms of the stress invariants p' and q:

$$\Psi = \left[\frac{p_{\mathrm{ref}}}{(2-\chi)K_0}V^{2-\chi} + \frac{q^2}{6p_{\mathrm{ref}}G_0}V^{-2\chi}\right] \qquad (1)^{a}$$

with

$$V = \frac{1}{2p_{\mathrm{ref}}}\left(3p' + \sqrt{p'^2 + \frac{2\chi K_0 q^2}{3G_0}}\right) \qquad (1)^{b}$$

Where K_0, G_0 and χ are material constants and p_{ref} denotes the atmospheric pressure. This formulation provides a thermodynamically consistent basis for deriving the hyperelastic stress–strain relations, where $p' = \frac{-tr\boldsymbol{\sigma}'}{3}$ denotes the mean effective stress and $q = \sqrt{\frac{3}{2}\boldsymbol{S}:\boldsymbol{S}}$ represents the deviatoric stress invariant, with $\boldsymbol{S}$ being the deviatoric part of the effective stress tensor $\boldsymbol{\sigma}'$. Accordingly, the elastic strain $\boldsymbol{\varepsilon}^{\mathrm{e}}$, compliance tensor $\mathbf{C}$ and the elastic stiffness tensor $\boldsymbol{E^e}$ are obtained directly from the energy potential as follows:

$$\boldsymbol{\varepsilon}^{\mathrm{e}} = \frac{\partial\Psi}{\partial\boldsymbol{\sigma}'} \;;\; \mathbf{C} = \frac{\partial^2\Psi}{\partial\boldsymbol{\sigma}'\partial\boldsymbol{\sigma}'} \;;\; \boldsymbol{E^e} = \mathbf{C}^{-1} \qquad (2)$$

2.2 Yield surface

In this study, the narrow-cone shaped yield surface proposed by Dafalias and Manzari (2004) is adopted. It can be expressed as:

$$f = [(\boldsymbol{S} - p'\boldsymbol{\alpha}):(\boldsymbol{S} - p'\boldsymbol{\alpha})]^{0.5} - \sqrt{\frac{2}{3}}p'm \qquad (3)$$

wherein m is a material constant defining half of the opening angle of the cone in stress space, $\boldsymbol{\alpha}$ is the back-stress ratio tensor representing kinematic hardening. The deviatoric unit tensor, which is normal to the yield surface, is obtained by differentiation of the yield function with respect to the stress tensor:

$$\frac{\partial f}{\partial\boldsymbol{\sigma}'} = \boldsymbol{n} - \frac{1}{3}(\boldsymbol{n}:\boldsymbol{r})\boldsymbol{I} \qquad (4)$$

Here $\boldsymbol{n} = \frac{\boldsymbol{r}-\boldsymbol{\alpha}}{\sqrt{2/3}m}$ and the deviatoric stress ratio $\boldsymbol{r} = \frac{\boldsymbol{S}}{p'}$.

2.3 Plastic strain and flow rule

The plastic strain rate $\dot{\boldsymbol{\varepsilon}}^{p}$ and non-associated flow rule $\boldsymbol{R}$ are adopted following the approach of Manzari and Dafalias (2004) and expressed as:

$$\dot{\boldsymbol{\varepsilon}}^{p} = \langle\dot{\lambda}\rangle\boldsymbol{R} \;;\; \dot{\lambda} = \frac{1}{\overline{K}}\,\boldsymbol{N}:\boldsymbol{E^e}:\dot{\boldsymbol{\varepsilon}} \qquad (5)$$

$\dot{\lambda}$ and $\boldsymbol{N}$ denote the plastic multiplier and loading direction, respectively. $\boldsymbol{R}$ includes the deviatoric part ($\boldsymbol{n}$) and isotropic part ($\boldsymbol{I}$). The sign and magnitude of the isotropic components are governed by the dilatancy D as follows (after Dafalias and Manzari 2004):

$$D = -A_d\left(\boldsymbol{\alpha}_\theta^d - \boldsymbol{\alpha}\right):\boldsymbol{n} \;;\; A_d = A_0(1 + \langle\boldsymbol{z}:\boldsymbol{n}\rangle) \qquad (6)$$

In this context, A_0 is the material parameter and $\boldsymbol{z}$ is the fabric dilatancy tensor. $\boldsymbol{\alpha}_\theta^d$ indicates phase transformation stress obliquities.

2.4 State parameter and fiber inclusion

The concept of the state parameter originally proposed by Been and Jefferies (1985) has been adopted in the benchmark model of Dafalias and Manzari. The state parameter (ψ) provides a simple yet powerful means of distinguishing between loose and dense soil states, as it accounts for the combined influence of void ratio (e) and effective stress on soil behavior. Specifically, soils with a positive state parameter exhibit contractive tendencies, whereas those with a negative value display dilative behavior. The concept thereby offers a unified framework for capturing density- and pressure-dependent responses. In the case of fiber-reinforced soils, however, the inclusion of discrete tensile elements alters the soil fabric and modifies the critical state characteristics (Karimzadeg et al., 2021). The reinforcing fibers influence the stress–strain response not only by contributing additional tensile resistance but also by altering the threshold

between dilative and contractive behavior. Consequently, the state of the soil cannot be fully described by stress and void ratio alone; the fiber content should also be incorporated. To address this, a modified state parameter is introduced, which extends the classical definition of Been and Jefferies to explicitly account for the effect of fiber inclusions. This enhanced formulation enables a more realistic description of the mechanical response of fiber-reinforced soils across a broad range of densities, confining stresses, and reinforcement ratios. The modified state parameter is expressed as:

$$\psi = e - e_{cs} - \left(\frac{\mathrm{FC}}{e_f + \mathrm{FC}}\right) \qquad (7)^{a}$$

with

$$e_{cs} = e_c - \lambda\left(\frac{p'}{p_{\mathrm{ref}}}\right)^{\zeta} \qquad (7)^{b}$$

In this concept, FC is the fiber content, e_f, e_c and ζ are material parameters. Modifying the state parameter directly influences the soil's mechanical response by altering the location of the critical state line, the magnitude of the peak stress ratio, and the dilatancy characteristics. In particular, the incorporation of fiber effects into the state parameter modifies the stress obliquities that govern peak α_θ^b, dilatancy α_θ^d and critical state α_θ^c. These dependencies are expressed through the following formulations:

$$\alpha_\theta^b = \boldsymbol{n}\sqrt{\frac{2}{3}}\left[g(\theta)M^c\exp\left(n^b\langle-\psi\rangle\right) - m\right]$$

$$\alpha_\theta^d = \boldsymbol{n}\sqrt{\frac{2}{3}}\left[g(\theta)M^c\exp\left(n^d\,\psi\right) - m\right] \qquad (8)$$

$$\alpha_\theta^c = \boldsymbol{n}\sqrt{\frac{2}{3}}\left[g(\theta)M^c - m\right]$$

Wherein $g(\theta) = 2c/((1+c) - (1-c)\cos 3\theta$ holds with $\cos 3\theta = \sqrt{6}\,tr(\boldsymbol{n}^3)$ and c is a material parameter. At the critical state, the stress ratio is characterized by the critical state stress obliquity M^c which remains constant for clean sand under triaxial compression. This constant value reflects the unique slope of the critical state line in the $q - p'$ plane, independent of density or initial stress history. In the case of fiber-reinforced soils, however, the inclusion of reinforcing elements modifies the soil fabric and its ability to mobilize shear resistance at large strains. As a result, the slope of the critical state line no longer remains constant but varies as a function of fiber content and the modified state parameter. This variation captures the experimentally observed strengthening effect of fibers, where the critical state shear resistance increases with reinforcement. The relationship can be mathematically expressed as:

$$M^c = \frac{q^{cs}}{p'^{cs}} + \left(\frac{\mathrm{FC}}{m_f + \mathrm{FC}}\right) \qquad (5)$$

wherein the mean effective and deviatoric stress state at the critical state are shown with p'^{cs} and q^{cs}, respectively. m_f is a material constant. The hyperbolic form of $\left(\frac{\mathrm{FC}}{m_f+\mathrm{FC}}\right)$ ensures that the effect of fibers increases monotonically with reinforcement but approaches an asymptotic value at high FC, thereby preventing unrealistic growth of shear strength. m_f controls the rate of this trend, with smaller values of m_f producing stronger reinforcement effects at lower fiber contents.

3 MODEL EVALUATION

To evaluate the performance of the proposed constitutive model, the triaxial test data of Ganiev et al. (2022) on polyvinyl alcohol (PVA)-reinforced sand were employed. In this experimental program, PVA fibers were incorporated at mass fractions of 0%, 2%, and 4% relative to the dry weight of sand. Specimens were prepared at different initial densities and sheared under a confining pressure of 100 kPa. Figure 1 presents a comparison between the model predictions and the corresponding experimental results. As shown in Figures 1(a) and 1(b), the model successfully reproduces both the peak deviatoric stress and the volumetric strain response of clean sand. With increasing fiber content up to 4%, the experimental data reveal a marked enhancement in deviatoric strength and a shift toward more dilative volumetric behavior. These trends are consistently captured by the proposed model, demonstrating its capability to represent the reinforcing effect of fibers within the bounding surface plasticity framework. The introduction of fiber content directly modifies the state parameter through the term FC/(e_f + FC), where ψ decreases as FC increases. This shift toward more negative values of ψ corresponds to a denser relative state, thereby promoting dilative tendencies. As a result, the bounding surface α_θ^b expands outward, reflecting an increase in peak strength and enhanced kinematic hardening, while the dilatancy surface α_θ^d contracts inward, indicating earlier initiation of dilation and stronger volumetric expansion during shear. From the proposed formulation, it is evident that increasing the FC increases the critical state stress ratio M^c. Physically, this corresponds to a steeper slope of the critical state line in $q - p'$ plane, reflecting the enhanced shear resistance imparted by fibers at large strains.

It is worth noting that, in simulating the series of fiber-reinforced soil tests, the fiber content was treated as a constant input parameter. However, in the case of root-reinforced soils, FC should more realistically be ex-

pressed as a function of root type, geometry, and diameter distribution. This distinction highlights the additional complexity involved
in extending the model from synthetic fibers to natural root systems.

4 CONCLUSIONS

This study presented a novel hyperelastic–plastic constitutive framework for simulating the behavior of fiber-reinforced soils. The model combines a hyperelastic formulation derived from an energy potential with a bounding surface plasticity theory, thereby ensuring energy conservation in the elastic domain of behavior. Unlike synthetic fibers, root systems introduce additional variability associated with root type, geometry, and distribution. Future extensions of the model will therefore incorporate these natural complexities, allowing for a more realistic representation of soil–root interactions under environmental and cyclic loading conditions. It is worth mentioning that under cyclic loading, if large strains occur during the first cycle (e.g., strains comparable to those observed in the triaxial tests shown in Figure 1), the roots may become damaged, potentially altering their behavior in subsequent cycles. This aspect requires further investigation.

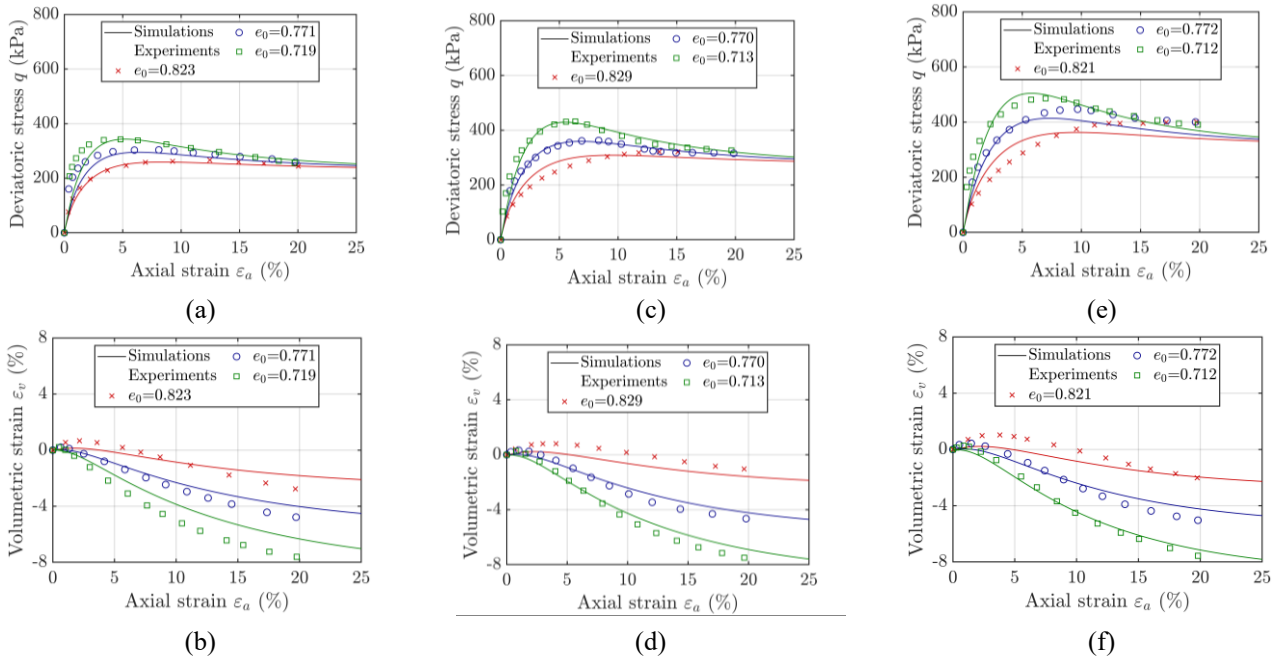

Figure 1. Comparison between model predictions and experimental data from Ganiev et al. (2022) on PVA-reinforced sand samples under an initial mean effective stress of $p'_0 = 100\ kPa$. (a) and (b) clean sand, (c) and (d) 2% fiber content, (e) and (f) 4% fiber content

5 REFERENCES

Been, K., Jefferies, M.G. 1985. A state parameter for sands, *Géotechnique* **35**(2), 99-112.

Dafalias, Y.F., Manzari, M.T. 2004. Simple plasticity sand model accounting for fabric change effects, *Journal of Engineering mechanics* **130**(6), 622-634.

Ganiev, J., Nakano, M., Sakai, T. 2022. Numerical analysis of drained compression behavior of fiber-reinforced sand based on a soil skeleton structure concept, *Computers and Geotechnics* **148**, 104789.

Gao, Z., Zhao, J. 2013. Evaluation on failure of fiber-reinforced sand, *Journal of Geotechnical and Geoenvironmental Engineering* **139**(1), 95-106.

Irani, N., Schmüdderich, C., Wichtmann, T. 2025. Application of a state-dependent hyperelastic-plastic constitutive model for slope stability analysis of fiber-reinforced sand. *E3S Web of Conferences* **642**, 02005. EDP Sciences.

Karimzadeh, A.A., Leung, A.K., Hosseinpour, S., Wu, Z., Fardad Amini, P. 2021. Monotonic and cyclic behaviour of root-reinforced sand, *Canadian Geotechnical Journal* **58**(12), 1915-1927.

Wood, D.M., Diambra, A., Ibraim, E. 2016. Fibers and soils: a route towards modelling of root-soil systems, *Soils and Foundations* **56**(5), 765-778.